



PREPARATION AND PHOTOCATALYTIC PROPERTIES OF Fe³⁺-DOPED TiO₂ NANOPARTICLES

Guoqiang Zhou^{[a][b]*}, Wenyang Wang^{[a][b]}, Baofeng Zheng^[a], Yang Li^[a]

Keywords: Photocatalytic property, Titanium dioxide, Iron doping, Acid red, Nanoparticles

The Fe³⁺-doped TiO₂ nanoparticles were synthesized by sol-gel method in an aqueous solution at a temperature of 160 °C. The effect of particle size, Fe³⁺-doping and dosage on the photocatalytic activity of the nanoparticles was investigated. The synthesized Fe³⁺-doped TiO₂ nanoparticles were analyzed by field emission scanning electron microscopy, transmission electron microscope, powder X-ray diffraction and dynamic light scattering. The nanoparticles had irregular shapes, and the primary size of particles was approximately 100 nm. Though the Fe³⁺-doping did not change the crystal structure of TiO₂, but it had significant affect on their photocatalytic properties. 0.5 % Fe³⁺-doped TiO₂ had the best photocatalytic performance. The particle size of Fe³⁺-doped TiO₂ samples also influenced its photocatalytic activity.

* Corresponding Authors

E-Mail: zhougq1982@163.com

[a] College of Chemistry and Environmental Science, Hebei University, Baoding, 071002, China

[b] Key Laboratory of Chemical Biology of Hebei Province, Hebei University, Baoding, 071002, China

Introduction

The photocatalytic technology is a new environmental technology gradually developed from the 1970s. The non-toxic, harmless and non-corrosive titanium dioxide (TiO₂) has been widely applied to the photodegradation of organic pollutants.¹ However, TiO₂ has a low photocatalytic efficiency due to the wide band-gap energy of TiO₂ (ca. 3.0 eV for rutile and 3.2 eV for anatase), and only the UV radiation range can be utilized well during the photocatalysis and there is relatively high rate of electron-hole recombinations.^{2,3} Therefore, improving the photocatalytic activity of TiO₂ seems to be an important area.

A great deal of research has focused on extending the ability of TiO₂ to avoid the recombination rate. The first alternative is modifying the TiO₂ surface using noble metals, the second alternative is to couple TiO₂ with another semiconductor having a favorable band gap, and the third alternative is to dope the TiO₂ with a transition metal ion, e.g. with Fe(III).⁴⁻⁶ Selective doping of TiO₂ with transition metal cations improved its photoactivity, while maintaining a good control of the primary particle size helped to achieve nanoscale configurations of the catalysts.^{7,8} Using Fe(III)-salts during the hydrolysis of Ti-salts the Fe(III) ions may replace titanium(IV) ions.⁹ Nagaveni prepared W, V, Ce, Zr, Fe, and Cu ion-doped anatase TiO₂ nanoparticles by a solution combustion method and found that the solid solution formation was limited to a narrow range of concentrations of the dopant ions.¹⁰

In this study, we report the preparation of Fe³⁺-doped TiO₂ nanoparticles via sol-gel synthesis method in an aqueous solution at a low temperature and examine the

influence of particle size, Fe³⁺-doping and dosage on the photocatalytic activity of the nanoparticles. The synthesized Fe³⁺-doped TiO₂ nanoparticles were characterized using X-ray diffraction (XRD), transmission electron microscope (TEM), field emission scanning electron microscopy (FE-SEM) and dynamic light scattering (DLS). The results showed that the Fe³⁺-doping improves the photocatalytic activity of the pure TiO₂ by reducing the recombination rate of electron-hole.

Experimental

Chemicals

All the chemicals used were analytical grade materials and used without further purification. Titanium tetrachloride (TiCl₄, 99%), iron (III) chloride hydrate (FeCl₃·6H₂O, 98%), hexadecyltrimethyl ammonium bromide (CTAB, 99%), and ammonia solution (25-28 % NH₃ in water) were obtained from Aladdin Chemical Reagent Co. Deionized water was used throughout the reactions. All glasswares were washed with dilute nitric acid (HNO₃) and distilled water, and dried in hot air oven.

Synthesis of Fe³⁺-doped TiO₂ nanoparticles

Fe³⁺-doped TiO₂ nanoparticles were synthesized as follows. A predetermined amount of FeCl₃·6H₂O was dissolved in 200 ml deionized water. The concentration of Fe³⁺ dopant was controlled between 0.1 and 1.0 wt. % of that of TiO₂. Then 15 ml titanium tetrachloride was added dropwise into FeCl₃·6H₂O aqueous solution under vigorous stirring. After that, a certain amount of surfactant CTAB was added into the solution. White paste was obtained after the pH value was adjusted to weakly alkaline using ammonia solution. The mixtures were then heated to 160 °C and kept at that temperature while being stirred for 6 h. The TiO₂ nanoparticles doped with 0.1 % Fe³⁺[R1], 0.3 % Fe³⁺, 0.5 % Fe³⁺ and 1.0% Fe³⁺ ions were prepared. Fe³⁺-doped TiO₂ bulky particles were obtained without adding CTAB according to the above synthetic process.

Characterization of nanoparticles

The particle size and shape of synthesized Fe³⁺-doped TiO₂ nanoparticles were measured by TEM (JEM-2010, JEOL, Japan). A minute drop of nanoparticles solution was cast on to a carbon-coated copper grid and subsequently dried in air before transferring it to the microscope. The morphology of synthesized nanoparticles was characterized using a FE-SEM (JSM-7500F, JEOL, Japan) operating at an acceleration voltage of 20 kV. The samples were prepared by sprinkling the powder on a double sided adhesive tape and mounting them on a microscope stub. Then the samples were coated with sputtered gold. The crystal phases of titania-based powders were studied by X-ray diffraction equipped with Cu K α X-Ray tubes operating at 40 kV and 50 mA (D8 Advance, Bruker, Germany). The 2 θ angle was varied from 20 to 60°. The size distribution of the nanoparticles in medium was evaluated by DLS (Delsa Nano C, Beckman, USA). Data were analyzed based on six replicated tests.

Photocatalytic activity assay

200 mL suspensions containing 50 mg L⁻¹ acid red dye and a certain quantity of Fe³⁺ doped TiO₂ nanoparticles were stirred in the dark for 30 min followed by sunlight exposure. The supernatant was taken at regular intervals and tested for the absorbance. The A- λ curve was scanned at full band by UV-visible spectrophotometer. The photocatalytic activity is expressed in degradation rate (Φ). The degradation rate was measured using the absorbance of dye solution at the maximum absorption wavelength. The degradation rate (Φ) was calculated by the following equation:

$$\Phi = \frac{A_0 - A}{A_0} \quad (1)$$

where, A_0 and A are the initial and final absorbance of the dye solution, respectively.

Results and discussion

Size and morphological investigation

TEM image of 0.5 wt. % Fe³⁺-doped TiO₂ nanoparticles are shown in Fig. 1. The Fe³⁺ doped TiO₂ nanoparticles are well dispersed with narrow size distribution. The TEM investigation indicates that the nanoparticles are aggregated particles with irregular shapes and the primary size is approximate 100 nm. The morphology of the 0.5 wt. % Fe³⁺-doped TiO₂ nanoparticles is observed in a SEM (Fig. 2). The SEM micrograph shows that the nanoparticles are made up of agglomeration of many primary particles, and have irregular shapes. The TEM image provides information on the primary size of nanoparticles, however, it could not provide information on whether the nanoparticles existed in single or aggregated forms in the aqueous solution. The size distribution in the aqueous solution, therefore, was investigated using a DLS method,

which shows that the average size of 0.5 wt. % Fe³⁺-doped TiO₂ nanoparticles in the aqueous solution is 105.4 \pm 23.2 nm (Fig. 3).

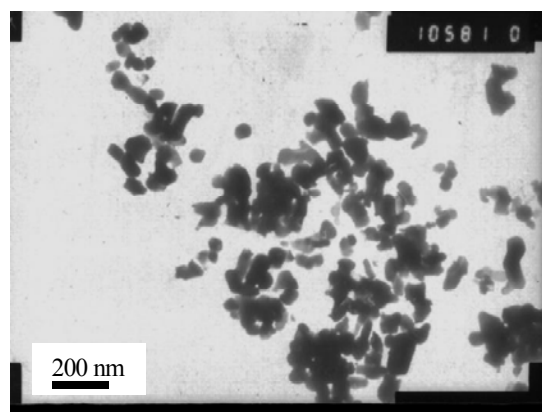


Figure 1. TEM micrograph of 0.5 % Fe³⁺-doped TiO₂ nanoparticles.

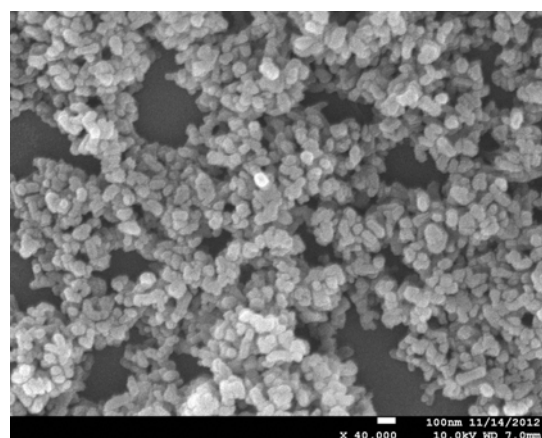


Figure 2. SEM image of 0.5 % Fe³⁺-doped TiO₂ nanoparticles.

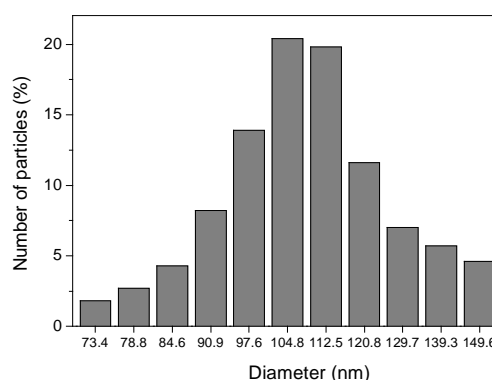


Figure 3. Size distribution of 0.5 % Fe³⁺-doped TiO₂ nanoparticles in aqueous solution measured by DLS.

The DLS analysis shows that the Fe³⁺-doped nanoparticles are homogeneously dispersed in aqueous solution. The fluid dynamics size of Fe³⁺-doped nanoparticles, measured by DLS, is in agreement with the primary size obtained by TEM.

XRD analysis

The XRD pattern of 0.5 wt. % Fe³⁺-doped TiO₂ powders is shown in Fig. 4. It can be seen that the sample exhibits the patterns associated to the crystalline anatase phase with peaks at 25.3°, 37.7°, 47.9°, and 54.2°, indicating that single phase anatase nanocrystallites are formed. The peaks at 2θ = 25.3°, 37.7°, 47.9°, and 54.2° can be attributed to the anatase (101), (004), (200) and (211) crystal planes, as previously reported.¹¹

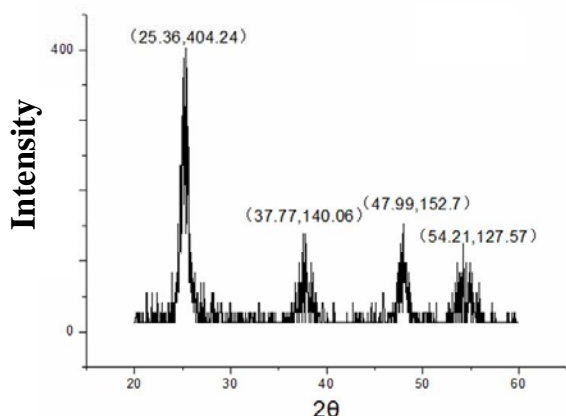


Figure 4. XRD patterns of 0.5 % Fe³⁺-doped TiO₂ samples.

No hints for the presence of other crystalline phases of TiO₂ (i.e., rutile and brookite) or segregated iron compounds like hematite (α-Fe₂O₃) and pseudobrookite (Fe₂TiO₅) were found in the X-ray diffractometry pattern. This is because the amount of iron ions added and the process temperature is low. It is reported that Fe₂O₃ and Fe₂TiO₅ were formed at high calcination temperature (the formation temperatures of Fe₂O₃ and Fe₂TiO₅ are 600 °C and 800 °C, respectively).¹² The results indicate that Fe³⁺ is homogeneously dispersed in the TiO₂ crystal lattice.

Effect of the particle size on photocatalytic activity

The effects of bulky and nano-Fe³⁺-doped TiO₂ particles on degradation rates of Acid Red solution are shown in Figure 5. The test conditions were: Acid Red = 50 mg L⁻¹, pH = 6.5, amount of doping Fe³⁺ in TiO₂ = 0.5 % and Fe³⁺-doped TiO₂ nanoparticles concentration = 1.5 g L⁻¹. As shown in Figure 5, only a small amount of Acid Red is degraded in sunlight without Fe³⁺-doped TiO₂ nanoparticles. The degradation of Acid Red is obvious after exposing Fe³⁺-doped TiO₂ nanoparticles. The Acid Red concentration is decreased rapidly within 40 min and the degradation rate keeps rising slowly as extension of reaction time. When the reaction time is 60 min, the degradation rate can reach to 74.04 %. However, the degradation effects of bulky Fe³⁺-doped TiO₂ particles on the Acid Red are lower than that of Fe³⁺-doped TiO₂ nanoparticles significantly at the same doping proportion. When the reaction time is 60 min, the degradation rate of Acid Red in the presence of bulky Fe³⁺-doped TiO₂ particles is 37.72 %. It may be that Fe³⁺-doped TiO₂ nanoparticles have large specific surface area and larger number of channels than bulky particles, which makes the nanoparticles, have higher catalytic activity.¹³

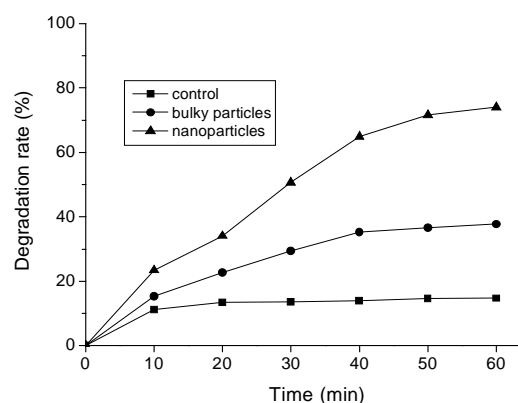


Figure 5. Effect of the particle size on photodegradation rate.

Effect of the amount of Fe³⁺-doping on photocatalytic activity

The degradation rates of Acid Red in the presence of Fe³⁺-doped TiO₂ nanoparticles with different amount of doping Fe³⁺ are shown in Fig. 6. The test conditions were: Acid Red = 50 mg L⁻¹, pH = 6.5 and Fe³⁺-doped TiO₂ nanoparticles = 1.5 g L⁻¹. As shown in Fig. 6, the photocatalytic efficiency of Fe³⁺-doped TiO₂ nanoparticles is higher than single TiO₂ nanoparticles. With increasing amount of Fe³⁺-doping, the photocatalytic efficiency shows a maximum. The optimal content of doped Fe³⁺ is 0.5 %. Since metal ions are effective electron acceptors, it may be that the doping Fe³⁺-ions build into the crystal lattice of TiO₂ and capture electrons in the conduction band of TiO₂. The competition of Fe³⁺ with electrons reduces the combination of electrons and number of holes on the surface of TiO₂. This produces more •OH radical on the surface of TiO₂ and improves the photocatalytic activity.^{14,15} Too little amount of doping Fe³⁺ can not capture electrons effectively, thus the catalytic effect is not as significant. Large amount of doping Fe³⁺ can act as a recombination center of electrons and holes. It will increase the combination probability of electrons and holes in the compound. Moreover, the Fe³⁺-doping may reach saturation and generate a new phase of Fe₂O₃ in the TiO₂. The Fe₂O₃ reduces the light intensity on the surface of the TiO₂, and leads to the decline of Acid Red degradation rate.^{16,17}

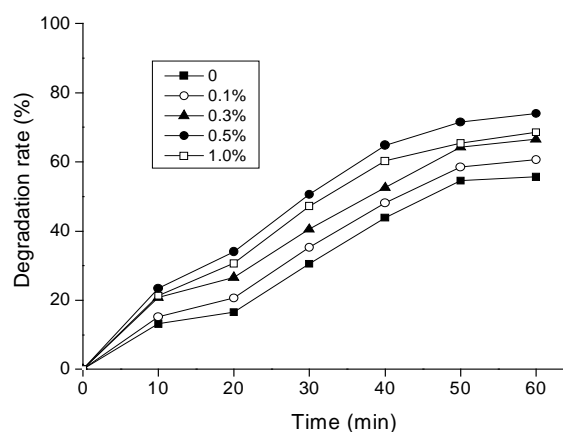


Figure 6. Effect of the amount of doping Fe³⁺ on photodegradation rate.

Effect of catalyst dosage on photocatalytic activity

The degradation rates of Acid Red in the presence of different dosage of Fe³⁺-doped TiO₂ nanoparticles are shown in Fig. 7. The test conditions were: Acid Red = 50 mg L⁻¹, pH = 6.5, and amount of doping Fe³⁺ in TiO₂ = 0.5 %. As shown in Fig. 7, the degradation rates of Acid Red increased with increasing catalyst dosage in a certain range. However, when the catalyst dosage reaches to 2.0 g L⁻¹, the degradation rates begins to decline.

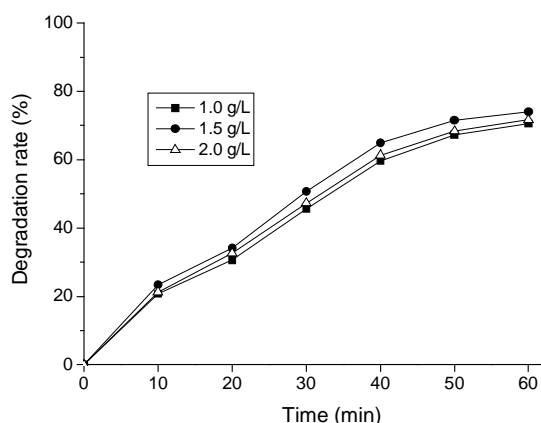


Figure 7. Effect of the dosage of nanoparticles on photodegradation rate

The catalytic activity of Fe³⁺-doped TiO₂ nanoparticles on the Acid Red photodegradation has a close relationship with its optical properties in solution.¹⁸ When the concentration is low, the catalytic activity is less due to the corresponding lower concentrations of reactive centers. Conversely, when the concentration is too high, the turbidity of solution is increased. Due to scattering of light on the particles in the solution, the light transmittance and utilization of incident light is decreased. These results lead to a reduction in the numbers of light induced hole-electron pairs, thereby reducing the degradation efficiency.

Conclusions

Photoactive Fe³⁺-doped TiO₂ nanoparticles were synthesized by sol-gel method at a low temperature of 160 °C. The results showed that the Fe³⁺-doping did not change the crystal structure of TiO₂, but significantly affected their photocatalytic properties. The XRD patterns, TEM and SEM images showed that the Fe³⁺-doped TiO₂ nanoparticles were single-phase anatase. 0.5% Fe³⁺ doped TiO₂ had the best photocatalytic activity among Fe³⁺-doped samples in Acid Red dye photodegradation. However, overloading of Fe³⁺ decreased the photocatalytic activity under visible light irradiation. The results could be explained by the balance of excited electrons/hole trapped by the doped Fe³⁺ and their charge recombination on the doped Fe³⁺ level. The particle size of Fe³⁺-doped TiO₂ also influenced the photocatalytic activity because it was found to be very large for the iron loaded sample compared with the reported values in the literature.

Acknowledgments

This research is financially supported by the National Natural Science Foundation of China (21001038) and the College Students Innovative Training Project of Hebei University (2013074).

References

- ¹Balázs, N., Mogyorósi, K., Srankó, D. F., Pallagi, A., Alapi, T., Oszkó, A., Dombi, A., Sipos, P., *Appl. Catal. B.*, **2008**, *84*, 356.
- ²Qi, K. H., Fei, B., Xin, J. H., *Thin. Solid. Films.*, **2011**, *519*, 2438.
- ³Veréb, G., Ambrus, Z., Pap, Z., Kmettykó, Á., Dombi, A., Danciu, V., Cheesman, A., Mogyorósi, K., *Appl. Catal. A.*, **2012**, *417*, 26.
- ⁴Vinu, R., Madras, G., *Appl. Catal. A.*, **2009**, *366*, 130.
- ⁵Teoh, W. Y., Amal, R., Mädler, L., Pratsinis, S. E., *Catal. Today.*, **2007**, *120*, 203.
- ⁶Bajnóczi, E. G., Balázs, N., Mogyorósi, K., Srankó, D. F., Pap, Zs., Ambrus, Z., Canton, S. E., Norén, K., Kuzmann, E., Vértes, A., Homonnay, Z., Oszkó, A., Pálkó, I., Sipos, P., *Appl. Catal. B.*, **2011**, *103*, 232.
- ⁷Yeung, K. L., Maira, A. J., Stolz, J., Hung, E., Hu, N. K. C., Wei, A. C., Soria, J., Cho, K. J., *J. Phys. Chem. B.*, **2002**, *106*, 4608.
- ⁸Li, X., Yue, P. L., Kutal, C., *New. J. Chem.*, **2003**, *27*, 1264.
- ⁹Choi, W., Termin, A., Hoffmann, M. R., *J. Phys. Chem. B.*, **1994**, *98*, 13669.
- ¹⁰Nagaveni, K., Sivalingam, G., Hegde, M. S., Madras, G., *Environ. Sci. Technol.*, **2004**, *38*, 1600.
- ¹¹Asilturk, M., Sayilkan, F., Arpac, E., *J. Photochem. Photobiol. A.*, **2009**, *203*, 64.
- ¹²Wang, Z. M., Yang, G., Biswas, P., Bresser, W., Boolchand, P., *Powder. Technol.*, **2001**, *114*, 197.
- ¹³Sharifi, S., Behzadi, S., Laurent, S., Forrest, M. L., Stroeve, P., Mahmoudi, M., *Chem. Soc. Rev.*, **2012**, *41*, 2323.
- ¹⁴Wang, C. Y., Böttcher, C. D., Bahnemann, W., Dohrmann, J. K., *J. Mater. Chem.*, **2003**, *13*, 2322.
- ¹⁵Wang, X. H., Li, J. G., Kamiyama, H., Moriyoshi, Y., Ishigaki, T., *J. Phys. Chem. B.*, **2006**, *110*, 6804.
- ¹⁶Souza, F. L., Lopes, K. P., Longo, E., Leite, E. R., *Phys. Chem. Chem. Phys.*, **2009**, *11*, 1215.
- ¹⁷Barroso, M., Mesa, C. A., Pendlebury, S. R., Cowan, A. J., Hisatomi, T., Sivula, K., Grätzel, M., Klug, D. R., Durrant, J. R., *Proc. Natl. Acad. Sci.*, **2012**, *109*, 15560.
- ¹⁸Beydoun, D., Amal, R., Low, G., McEvoy, S., *J. Nanopart. Res.*, **1999**, *1*, 439.

Received: 04.09.2013.

Accepted: 12.09.2013.